Electronic circular dichroism with real time time dependent density functional theory: Propagator formalism and gauge dependence

Mattiat, J ; Luber, Sandra

Abstract: Linear response theory is reviewed in a propagator formalism to treat linear response and real time (RT) time dependent density functional theory (TDDFT) in a common framework for the calculation of linear response tensors. The importance of an additional term in the definition of the momentum for a description in the velocity representation as well as an origin independent linear magnetic response in the presence of non-local pseudo potentials is discussed. The origin and meaning of the terms 'representation' and 'gauge' are explored and simulations of absorption and electronic circular dichroism spectra using RT-TDDFT are presented. The calculation of the electro-magnetic linear response functions has been implemented into the package CP2K using the gaussian and (augmented) plane wave method.

DOI: https://doi.org/10.1016/j.chemphys.2019.110464

Graphical Abstract

Electronic circular dichroism with real time time dependent density functional theory: Propagator formalism and gauge dependence

J. Mattiat, S. Luber[1]

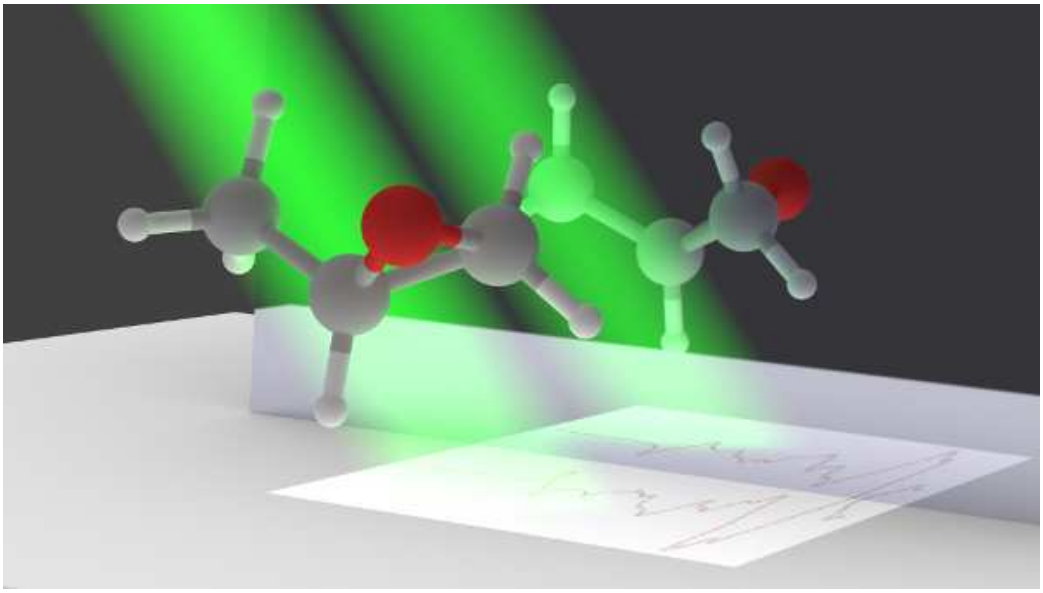

[1]E-Mail: sandra.luber@chem.uzh.ch

Highlights

Electronic circular dichroism with real time time dependent density functional theory: Propagator formalism and gauge dependence

J. Mattiat, S. Luber[2]

- Propagator formulation of linear response, treating LR- and RT-TDDFT on equal footing.
- Length/mixed/velocity forms of the electric-dipole–electric-dipole polarizability.
- Length/velocity form of the electric-dipole–magnetic-dipole polarizability in RT-TDDFT.
- Origin independent calculation of ECD spectra with non-local potentials in RT-TDDFT.
- Calculation of the polarizability tensors implemented in the CP2K package.

[2]E-Mail: sandra.luber@chem.uzh.ch

Electronic circular dichroism with real time time dependent density functional theory: Propagator formalism and gauge dependence

J. Mattiat, S. Luber[1]

University of Zurich, Department of Chemistry, Winterthurerstrasse 190, Zurich, Switzerland

Abstract

Linear response theory is reviewed in a propagator formalism to treat linear response and real time (RT) time dependent density functional theory (TDDFT) in a common framework for the calculation of linear response tensors. The importance of an additional term in the definition of the momentum for a description in the velocity representation as well as an origin independent linear magnetic response in the presence of non-local pseudo potentials is discussed. The origin and meaning of the terms 'representation' and 'gauge' are explored and simulations of absorption and electronic circular dichroism spectra with RT-TDDFT are presented. The calculation of the electro-magnetic linear response functions has been implemented into the package `CP2K` using the gaussian and (augmented) plane wave method.

Keywords: real time propagation, electronic circular dichroism, gauge invariance, origin independence, pseudo potentials, time-dependent density functional theory

1. Introduction

Starting with Yabana's and Bertsch's application of real time propagation techniques in the local density approximation of Kohn–Sham density functional theory (KS-DFT) [1] to the calculation of spectroscopic properties [2, 3], subsequent work showed the advantages and versatility of real

[1]E-Mail: sandra.luber@chem.uzh.ch

time time dependent density functional theory (RT-TDDFT). Later Yabana presented two implementations of RT-TDDFT, one in the length gauge (LG) and the other in the velocity gauge (VG) [4] for the application to infinitely periodic systems. The latter only gained wider attention recently [5, 6, 7].

Notable applications of RT-TDDFT to spectroscopy include, among others, the description of absorption spectra [8, 9], plasmon resonance [10, 11], Raman spectra [12, 13, 14, 15], electronic circular dichroism (ECD) spectra[16, 17], relativistic two- and four component KS-DFT [18, 19] [20], dielectric response of dye molecules on nano particles [21] and core level X-ray absorption [19] [22, 23, 24, 25], excited state absorption [26], and even non-linear protocols [27]. Reviews of RT-TDDFT can be found e. g. in Refs. [28, 29].

In many modern quantum chemistry packages pseudo potentials are used to describe core electrons in order to allow faster simulation times and to exploit the advantages of a plane wave grid in reciprocal space, respectively. The presence of non-local potentials complicates the simulation of the interaction of the system of interest with electro-magnetic fields, especially if a description of magnetic phenomena, such as ECD, is desired. Here the operators have to be transformed appropriately to a pseudo potential representation [30, 31], in order to retain gauge invariance of the description via the time dependent Kohn–Sham (TDKS) equations [32].

Simulations of ECD spectra are challenging, because the electric-dipole–magnetic-dipole tensor in the standard formulation (length representation) is origin dependent and the ECD spectra show also an origin dependence which only vanishes in the complete basis set limit. Two widely known strategies to overcome this problem have been suggested: 1. The use of London atomic orbitals [33, 34, 35, 36], which include a term dependent on the vector potential in the description of the atomic orbitals. 2. Switching to the velocity representation of the electric-dipole–magnetic-dipole tensor, which leads to origin independent ECD spectra [37]. In the framework of linear response (LR-) TDDFT, the length, mixed, and velocity representation of the electric-dipole–electric-dipole linear response tensor (polarizability) or the length and velocity representation of the electric-dipole–magnetic-dipole tensor are well known concepts [38, 39, 40, 41, 42, 43, 44, 45][46], and their relation to each other and to the choice of gauge has a long history [47, 48, 49, 50, 51, 52, 53]. Of course, the use of non-local pseudo potentials induces another layer of complexity.

This work uses the propagator formulation of linear response theory in

order to treat LR- and RT-TDDFT on equal footing. Additionally, it covers the complications introduced by the use of non-local pseudo potentials for the calculation of absorption and ECD spectra and presents a way to achieve gauge invariant and origin independent results for the simulation of linear response spectroscopy within RT-TDDFT.

After presenting the linear response theory framework in Sec. 2.1, its application to the simulation of absorption spectroscopy is given in Sec. 2.2. In Sec. 2.2.1 the Thomas–Reiche–Kuhn sum rules is discussed for absorption spectra calculated with non-local potentials. In Sec. 2.3 the length and velocity gauges are reviewed and in Sec. 2.4 the application to linear response theory for the simulation of ECD spectra is given with special emphasis on non-local pseudo potentials and origin independence. A short overview on the implementation and computational details of the calculations is given in Sec. 3. The implications of the theory presented in Sec. 2 are discussed in detail for the simulation of absorption spectra in Sec. 4.1 and ECD spectra in Sec. 4.2. Finally, a summary of the most important findings is given in Sec. 5.

2. Theory

For the sake of brevity the unperturbed, non-relativistic electronic Hamiltonian can be written as

$$\hat{H}_0 = \frac{\hat{p}^2}{2m_e} + \hat{V}^{\mathrm{loc}} + \hat{V}^{\mathrm{nl}} \tag{1}$$

where $\hat{V}^{\mathrm{loc}}$ groups all local potentials and $\hat{V}^{\mathrm{nl}}$ stands for non-local potentials, e. g. for the non-local part of pseudo potentials. $\hat{p}$ is the canonical momentum operator which is related to the position operator $\hat{r}$ by the canonical commutator relations

$$[\hat{r}_\alpha, \hat{p}_\beta] = i\hbar\delta_{\alpha\beta}, \qquad [\hat{p}_\alpha, \hat{p}_\beta] = [\hat{r}_\alpha, \hat{r}_\beta] = 0. \tag{2}$$

Greek indices denote the (x, y, z)-components of tensors throughout this work. The Einstein summation convention is assumed. The formula for the velocity representation (or 'form') of electric transition dipole moments is usually derived by the commutator relation

$$\left[\hat{r}_\alpha, \hat{H}_0\right] = \frac{i\hbar}{m_e}\hat{p}_\alpha + \left[\hat{r}_\alpha, \hat{V}^{\mathrm{nl}}\right]. \tag{3}$$

Thus, the electric transition dipole moment between two electronic energy eigenstates $|a\rangle$ and $|b\rangle$ of $\hat{H}_0$ becomes

$$(E_b - E_a)\,\langle a|{-e\hat{r}_\alpha}|b\rangle = \frac{-ie\hbar}{m_e}\,\langle a|\hat{p}_\alpha|b\rangle + \left\langle a\middle|\left[-e\hat{r}_\alpha, \hat{V}^{\mathrm{nl}}\right]\middle|b\right\rangle \tag{4}$$

where e is the elementary charge, $\hbar$ is the reduced Planck constant, m_e the rest mass of an electron, and E_a and E_b are the electronic energies belonging to states $|a\rangle$ and $|b\rangle$. In the following section a different angle on the velocity representation is provided in terms of propagators (or linear response functions) [54].

2.1. Propagator formulation of linear response

In general, spectroscopic properties can be obtained from (linear and non linear) response functions [55]. The linear (time domain) response function for observable $\hat{B}$ with respect to a time-dependent perturbation

$$\hat{H}_1(t) = -\hat{A}f(t) \tag{5}$$

is implicitly defined by [56]

$$\langle \hat{B}(t) \rangle - \langle \hat{B} \rangle_0 = \int_{-\infty}^{t} \mathrm{d}t' \ \langle\langle \hat{B}(t); \hat{A}(t') \rangle\rangle f(t') \tag{6}$$

where the propagator notation $\langle\langle \cdot; \cdot \rangle\rangle$ for the linear response function is adapted from Ref. [54]. Under the assumption that perturbations are applied independently from each other, the linear response function only depends on time differences $t - t'$ [56]. The time dependence of $\hat{A}$ in the linear response function is thus to be understood as to state that it is applied at the time t' with the explicit time dependence given by $f(t')$. The notation $\langle \cdot \rangle$ is used for the expectation value of $\hat{B}$,

$$\langle \hat{B}(t) \rangle = \mathrm{Tr}[\rho(t)\hat{B}]. \tag{7}$$

Here $\rho(t)$ is the time-dependent density matrix. $\langle \hat{B} \rangle_0$ denotes that the density matrix is the stationary one (ρ_0, i. e. the solution of the unperturbed problem, Eq. (1)).
Utilizing the properties of Fourier transforms (FTs), taking care of causality and introducing a damping factor ϵ in order to switch on the perturbation adiabatically leads to the frequency domain representation of the linear response function [56]

$$\langle\langle \hat{B}; \hat{A} \rangle\rangle_\omega = \langle \hat{B}(\hbar\omega) \rangle / f(\hbar\omega) \tag{8}$$

which forms a FT pair with its time domain representation. Note that here the subscript ω is used to denote the energy/frequency domain; in order to have consistent units it should be $\hbar\omega$. Here

$$\langle \hat{B}(\hbar\omega) \rangle = \lim_{\epsilon \to 0^+} \int_{-\infty}^{\infty} \mathrm{d}t \ \left(\langle \hat{B}(t) \rangle - \langle \hat{B} \rangle_0 \right) e^{i(\hbar\omega)/\hbar \, t} e^{-\epsilon t} \tag{9}$$

and $f(\hbar\omega)$ is the FT of $f(t)$. Eq. (8) is the working equation for linear response in RT-TDDFT: The linear response function is obtained essentially by tracking the time evolution of the desired observable with respect to a perturbation and taking the Fourier transform (in this work, this process is henceforth referred to as 'measurement').
In linear response, both a time domain (*Kubo formula*) [57]

$$\langle\langle \hat{B}(t); \hat{A}(t') \rangle\rangle = -\frac{i}{\hbar} \theta(t - t') \left\langle \left[\hat{B}(t), \hat{A}(t') \right] \right\rangle \tag{10}$$

and a frequency domain representation [54]

$$\langle\langle \hat{B}; \hat{A} \rangle\rangle_\omega = \lim_{\epsilon \to 0} \sum_n \frac{1}{\hbar} \left[\frac{\langle 0|\hat{B}|n\rangle \ \langle n|\hat{A}|0\rangle}{\omega - (\omega_n - \omega_0) + i\epsilon} - \frac{\langle 0|\hat{A}|n\rangle \ \langle n|\hat{B}|0\rangle}{\omega - (\omega_0 - \omega_n) - i\epsilon} \right] \tag{11}$$

of the propagator (or linear response function) can be derived. The latter is the equation which is solved for in LR-TDDFT, most commonly in either Casida's [58] or Sternheimer's [59] formalism. Note, that both of these expressions (Eqs. (10) and (11)) do not include any reference to the functional form of the perturbation $f(t)$ and only carry the assumption that it is weak. The following equivalent equations of motion hold for the frequency domain propagator [54]:

$$\begin{aligned}\hbar\omega\langle\langle\hat{A};\hat{B})\rangle\rangle_\omega &= \langle[\hat{A},\hat{B}]\rangle_0 + \langle\langle[\hat{A},H];\hat{B}\rangle\rangle_\omega \\ &= \langle[\hat{A},\hat{B}]\rangle_0 + \langle\langle A;[H,\hat{B}]\rangle\rangle_\omega.\end{aligned} \tag{12}$$

This equation provides a natural way to apply length, mixed and velocity representations [60] in RT- and LR-TDDFT as will be shown in the following. It is important to note that the commutator relations used in Eq. (12) are only valid for a complete basis set [37].

2.2. Length, mixed, and velocity representations of the electric-dipole–electric-dipole polarizability in the propagator formulation

The electric-dipole–electric-dipole polarizability $\alpha_{\alpha\beta}$ is related to the propagator $\langle\langle\hat{r}_\alpha;\hat{r}_\beta\rangle\rangle_\omega$ as [61]

$$\alpha_{\alpha\beta}(\hbar\omega) = -e^2\langle\langle\hat{r}_\alpha;\hat{r}_\beta\rangle\rangle_\omega \tag{13}$$

and the absorption strength function $S(\hbar\omega)$ is thus [62]

$$S(\hbar\omega) = \frac{-2m_e\omega}{3\pi\hbar}\mathrm{Tr}\left\{\mathrm{Im}\left[\langle\langle\hat{r}_\alpha;\hat{r}_\beta\rangle\rangle_\omega\right]\right\} \tag{14}$$

Applying Eq. (12) for the Hamiltonian in Eq. (1) to Eq. (13) one arrives at the following relations for the mixed representations

$$\hbar\omega\langle\langle\hat{r}_\alpha;\hat{r}_\beta\rangle\rangle_\omega = \left\langle\left\langle\frac{i\hbar}{m_e}\hat{p}_\alpha + [\hat{r}_\alpha,\hat{V}^{\mathrm{nl}}];\hat{r}_\beta\right\rangle\right\rangle_\omega = \frac{i\hbar}{m_e}\langle\langle\hat{p}^{\mathrm{gen}}_\alpha;\hat{r}_\beta\rangle\rangle_\omega = -\frac{i\hbar}{m_e}\langle\langle\hat{r}_\alpha;\hat{p}^{\mathrm{gen}}_\beta\rangle\rangle_\omega \tag{15}$$

and the velocity representation

$$\begin{aligned}\hbar^2\omega^2\langle\langle\hat{r}_\alpha;\hat{r}_\beta\rangle\rangle_\omega &= \left\langle\frac{\hbar^2}{m_e}\delta_{\alpha\beta} + [[\hat{r}_\alpha,\hat{V}^{\mathrm{nl}}],\hat{r}_\beta]\right\rangle_0 + \left\langle\left\langle\frac{i\hbar}{m_e}\hat{p}_\alpha + [\hat{r}_\alpha,\hat{V}^{\mathrm{nl}}];-\frac{i\hbar}{m_e}\hat{p}_\beta - [\hat{r}_\beta,\hat{V}^{\mathrm{nl}}]\right\rangle\right\rangle_\omega \\ &= \left\langle\frac{\hbar^2}{m_e}\delta_{\alpha\beta} + [[\hat{r}_\alpha,\hat{V}^{\mathrm{nl}}],\hat{r}_\beta]\right\rangle_0 + \frac{\hbar^2}{m_e^2}\langle\langle\hat{p}^{\mathrm{gen}}_\alpha;\hat{p}^{\mathrm{gen}}_\beta\rangle\rangle_\omega\end{aligned} \tag{16}$$

of the electric-dipole–electric-dipole polarizability. The modified definition of the momentum operator $\hat{p}^{\mathrm{gen}}$ will be called *generalized momentum* in this work (not to be confused with the term generalized momentum used in Lagrangian dynamics to denote the derivative of the Lagrangian with respect to the velocity):

$$\hat{p}_\alpha^{\mathrm{gen}} = \frac{m_e}{i\hbar}[\hat{r}_\alpha, \hat{H}] = \hat{p}_\alpha + \frac{m_e}{i\hbar}[\hat{r}_\alpha, \hat{V}^{\mathrm{nl}}]. \tag{17}$$

If there are no non-local potentials, of course $\hat{p}_\alpha^{\mathrm{gen}} = \hat{p}_\alpha$.

This formulation has the advantage of being immediately applicable to RT-TDDFT: A perturbation in the electric dipole approximation ($\hat{A} = -e\hat{r}$) and a measurement (i. e. tracking of the time evolution) of the electric dipole moment gives $\langle\langle \hat{r}_\alpha; \hat{r}_\beta \rangle\rangle_\omega$ via Eq. (8), while a measurement of the (generalized) momentum $\hat{p}^{\mathrm{gen}}$ gives $\langle\langle \hat{p}_\alpha^{\mathrm{gen}}; \hat{r}_\beta \rangle\rangle_\omega$. An overview over the different representations is given in Tab. 1. Note that according to Eq. (12) in a calculation of the electric-dipole–electric-dipole polarizability in either mixed or velocity representation the generalized momentum is necessary in the presence of non-local pseudo potentials.

propagator	measurement	perturbation
$\langle\langle \hat{r}_\alpha; \hat{r}_\beta \rangle\rangle_\omega$	$\hat{r}_\alpha$	$\hat{r}_\beta$
$\langle\langle \hat{r}_\alpha; \hat{p}_\beta^{\mathrm{gen}} \rangle\rangle_\omega$	$\hat{r}_\alpha$	$\hat{p}_\beta^{\mathrm{gen}}$
$\langle\langle \hat{p}_\alpha^{\mathrm{gen}}; \hat{r}_\beta \rangle\rangle_\omega$	$\hat{p}_\alpha^{\mathrm{gen}}$	$\hat{r}_\beta$
$\langle\langle \hat{p}_\alpha^{\mathrm{gen}}; \hat{p}_\beta^{\mathrm{gen}} \rangle\rangle_\omega$	$\hat{p}_\alpha^{\mathrm{gen}}$	$\hat{p}_\beta^{\mathrm{gen}}$

Table 1: Different representations of the propagators for an RT-TDDFT calculation of the electric-dipole–electric-dipole response tensor including non-local potentials. The propagators are related to each other according to Eqs. (15) and (16).

2.2.1. Thomas–Reiche–Kuhn sum rule

The absorption strength function Eq. (14) fullfills the Thomas–Reiche–Kuhn (TRK) sum rule [62, 60]

$$\int_0^\infty \mathrm{d}(\hbar\omega)\ S(\hbar\omega) = N_e \tag{18}$$

where N_e is the number of electrons in the system.

As pointed out by Starace [52] the sum rule for the absorption strength function has to be adapted when non-local potentials are used:

$$\int_0^\infty \mathrm{d}(\hbar\omega)\ S(\hbar\omega) = N_e + \frac{m_e}{3\hbar^2}\mathrm{Tr}\left\{\left\langle\left[\hat{r}_\alpha, \left[\hat{V}^{\mathrm{nl}}, \hat{r}_\beta\right]\right]\right\rangle_0\right\} \tag{19}$$

2.3. Length and velocity gauge

The starting point for the description of the interaction between electromagnetic radiation and a molecular system is usually the minimal coupling Hamiltonian in a semi-classical approximation (fields classically, system quantum mechanically) [63]

$$\hat{H} = \frac{1}{2m_e}\left(\hat{p}_\alpha + \frac{e}{c}A_\alpha(\vec{r},t)\right)^2 - eU(\vec{r},t) + \hat{V}^{\mathrm{loc}}(\vec{r}) \tag{20}$$

where $A_\alpha(\vec{r},t)$ are the components of the vector potential and $U(\vec{r},t)$ is the scalar potential, and the $\vec{r}$ and t dependence are explicitly denoted. The time-dependent perturbing part of this Hamiltonian has up to quadratic terms in A:

$$\hat{H}_1(t) = \frac{e}{m_e c}\hat{p}_\alpha A_\alpha(\vec{r},t) + \frac{e^2}{2m_e c^2}A(\vec{r},t)^2 - eU(\vec{r},t). \tag{21}$$

In most cases one reverts to the long wave approximation, where one assumes that the vector potential is constant in space over the system size $A_\alpha(\vec{r},t) = A_\alpha(t)$. The magnetic field vanishes in the long wave approximation. The description of the system in the KS-framework is gauge invariant [64, 32] under a gauge transformation [65]

$$\begin{aligned} A'_\alpha(t) &= A_\alpha(t) + \nabla\chi(\vec{r},t) \\ U'(t) &= U(t) - \frac{1}{c}\frac{\partial\chi(\vec{r},t)}{\partial t} \\ \hat{O}'(t) &= e^{\frac{ie}{c\hbar}\chi(\vec{r},t)}\hat{O}e^{-\frac{ie}{c\hbar}\chi(\vec{r},t)} \\ \Psi'(\vec{r},t) &= e^{\frac{ie}{c\hbar}\chi(\vec{r},t)}\Psi(\vec{r},t) \end{aligned} \tag{22}$$

where the scalar function $\chi(\vec{r},t)$ can be chosen freely, $\Psi(\vec{r},t)$ is any wave function and $\hat{O}$ a generic operator. A common gauge transformation is the Göppert-Mayer gauge transformation [66] with $\chi(\vec{r},t) = -\hat{r}_\alpha A_\alpha(t)$. This transformation has the effect that the vector potential vanishes and the perturbation Hamiltonian becomes linear in the electric field perturbation

$$\hat{H}'_1(t) = -e\hat{r}_\alpha E_\alpha(t) \tag{23}$$

where $E_\alpha(t)$ are the components of the electric field. This well-known expression is usually referred to as electric *dipole approximation* [67].

In (RT-)TDDFT there are two common choices of gauge [32]: 1. The length gauge (LG), where the perturbation is described by Eq. (23) and $A_\alpha^{\mathrm{LG}} = 0$, and 2. the velocity gauge (VG), where the perturbation is described by Eq. (21) with $U^{\mathrm{VG}} = 0$.

The formulae for the different representations of the electric-dipole–electric-dipole polarizability presented in Sec. 2.1 are not applicable to the perturbation described in Eq. (21), since it contains a term which is quadratic in the perturbation [63]. However, if the perturbation is sufficiently weak, the quadratic term may be neglected. In that case, up to linear response, the length, mixed and velocity representations actually are related to a description in the length and velocity gauge in the following way: The propagator (or linear response function) in the VG corresponds to a perturbation proportional to the momentum $\langle\langle \cdot; \hat{p}_\beta \rangle\rangle$ and thus gives the mixed or velocity representation, depending on the measurement.
Nonetheless, length and velocity representation (or form) and length and velocity gauge are not the same, if a description beyond linear response is required.
A disussion of length and velocity representations in LR-TDDFT and their role in a description beyond the dipole approximation can be found in Ref. [68].

2.4. Electric-dipole–magnetic-dipole polarizabilty (ECD)

The ECD spectrum is related to the electric-dipole–magnetic-dipole polarizabilty [61]

$$G_{\alpha\beta} = -e\langle\langle \hat{m}_\alpha; \hat{r}_\beta \rangle\rangle_\omega \tag{24}$$

via the rotatory strength function [17] (in atomic units)

$$R(\hbar\omega) = -\frac{1}{\pi}\mathrm{Tr}\left\{\mathrm{Re}\left[\langle\langle \hat{m}_\alpha; \hat{r}_\beta \rangle\rangle_\omega\right]\right\} \tag{25}$$

where the magnetic dipole moment $\hat{m}$ is defined as (neglecting spin and g factor) [69]

$$\hat{m}_\alpha = -\frac{e}{2m_e}\hat{l}_\alpha = -\frac{e}{2m_e}\epsilon_{\alpha\beta\gamma}\hat{r}_\beta\hat{p}_\gamma \tag{26}$$

where $\hat{l}_\alpha$ is the angular momentum operator and $\epsilon_{\alpha\beta\gamma}$ is the totally antisymmetric (Levi–Civita) tensor. It was shown that in the presence of non local potentials a modified version of the angular momentum operator in Eq. (26) is required in order to ensure gauge invariance [70, 31]. The modification demands the use of the generalized instead of the canonical momentum in Eq. (26) to first order in an applied magnetic field [30]:

$$\hat{m}^{\mathrm{gen}}_\alpha = -\frac{e}{2m_e}\epsilon_{\alpha\beta\gamma}\hat{r}_\beta\hat{p}^{\mathrm{gen}}_\gamma. \tag{27}$$

For a consistent terminology this definition is called here *generalized magnetic dipole moment* and has to be used also if the magnetic field vanishes, as in

the long wave approximation, if a gauge invariant description of magnetic phenomena is to be achieved [16, 71].

Applying Eq. (12) for a Hamiltonian of the form in Eq. (1) to the linear response function in Eq. (24) gives

$$\begin{aligned}\hbar\omega\langle\langle\hat{m}_\alpha^{\mathrm{gen}};\hat{r}_\beta\rangle\rangle_\omega =&\langle[\hat{m}_\alpha^{\mathrm{gen}},\hat{r}_\beta]\rangle_0+\langle\langle\hat{m}_\alpha^{\mathrm{gen}};[\hat{H}_0,\hat{r}_\beta]\rangle\rangle_\omega\\ =&\frac{-e}{2m_e}\left\langle\epsilon_{\alpha\beta\gamma}i\hbar\hat{r}_\gamma+\epsilon_{\alpha\gamma\delta}\frac{m_e}{i\hbar}\hat{r}_\gamma\left[\left[\hat{r}_\delta,\hat{V}^{\mathrm{nl}}\right],\hat{r}_\beta\right]\right\rangle_0-\frac{i\hbar}{m_e}\langle\langle\hat{m}_\alpha^{\mathrm{gen}};\hat{p}_\beta^{\mathrm{gen}}\rangle\rangle_\omega.\end{aligned} \tag{28}$$

In Tab. 2 the length and velocity representation of the electric-dipole–magnetic-dipole tensor are listed, which are related by Eq. (28). Of course, also a magnetic perturbation could be applied while measuring either the electric dipole moment or generalized momentum giving response functions of the form $\langle\langle\cdot;\hat{m}_\beta^{\mathrm{gen}}\rangle\rangle_\omega$. However this would require a description beyond the electric dipole approximation which was not carried out in this work.

propagator	measurement	perturbation
$\langle\langle\hat{m}_\alpha^{\mathrm{gen}};\hat{r}_\beta\rangle\rangle_\omega$	$\hat{m}_\alpha^{\mathrm{gen}}$	$\hat{r}_\beta$
$\langle\langle\hat{m}_\alpha^{\mathrm{gen}};\hat{p}_\beta^{\mathrm{gen}}\rangle\rangle_\omega$	$\hat{m}_\alpha^{\mathrm{gen}}$	$\hat{p}_\beta^{\mathrm{gen}}$

Table 2: Different representations of the propagators for an RT-TDDFT calculation of the electric-dipole–magnetic-dipole response tensor including non-local potentials. The propagators are related to each other according to Eq. (28).

2.4.1. Origin dependence

As opposed to the electric-dipole–electric-dipole tensor the electric-dipole–magnetic-dipole tensor $G_{\alpha\beta}$ is origin dependent [69], which stems essentially from the dependence of the angular momentum operator $\hat{l}_\alpha$ under a shift of origin $O\to O+a$ (according to Eq. (27))

$$\hat{m}_\alpha^{\mathrm{gen},O+a}=\hat{m}_\alpha^{\mathrm{gen},O}+\frac{e}{2m_e}\epsilon_{\alpha\beta\gamma}a_\beta\hat{p}_\gamma^{\mathrm{gen}} \tag{29}$$

In principle, experimental observables, as e. g. the ECD spectrum, should be invariant under such a shift. However, as amply discussed in literature magnetic linear response calculations show an origin dependence if an incomplete basis set is used [72, 73, 74, 61, 37, 16]. Common approaches to this difficulty are either London atomic orbitals [33] or a description in the velocity representation [37]. In this work the latter will be discussed in a

RT-TDDFT framework. Explicitly calculating the origin dependence of the electric-dipole–magnetic-dipole tensor in the length representation gives according to Eqs. (11) and (29)

$$\langle\langle \hat{m}_\alpha^{\mathrm{gen},O+a}; \hat{r}_\beta^{O+a} \rangle\rangle_\omega = \langle\langle \hat{m}_\alpha^{\mathrm{gen},O}; \hat{r}_\beta \rangle\rangle_\omega + \frac{e}{2m_e} \epsilon_{\alpha\gamma\delta} a_\gamma \langle\langle \hat{p}_\delta^{\mathrm{gen}}; \hat{r}_\beta \rangle\rangle_\omega \tag{30}$$

and thus for the trace in Eq. (25)

$$\begin{aligned}
\sum_\alpha \langle\langle \hat{m}_\alpha^{\mathrm{gen},O+a}; \hat{r}_\alpha^{O+a} \rangle\rangle_\omega = &\sum_\alpha \langle\langle \hat{m}_\alpha^{\mathrm{gen},O}; \hat{r}_\alpha \rangle\rangle_\omega \\
&+ \frac{e}{2m_e} \left(a_y \langle\langle \hat{p}_z^{\mathrm{gen}}; \hat{r}_x \rangle\rangle_\omega - a_z \langle\langle \hat{p}_y^{\mathrm{gen}}; \hat{r}_x \rangle\rangle_\omega \right) \\
&+ \frac{e}{2m_e} \left(a_z \langle\langle \hat{p}_x^{\mathrm{gen}}; \hat{r}_y \rangle\rangle_\omega - a_x \langle\langle \hat{p}_z^{\mathrm{gen}}; \hat{r}_y \rangle\rangle_\omega \right) \\
&+ \frac{e}{2m_e} \left(a_x \langle\langle \hat{p}_y^{\mathrm{gen}}; \hat{r}_z \rangle\rangle_\omega - a_y \langle\langle \hat{p}_x^{\mathrm{gen}}; \hat{r}_z \rangle\rangle_\omega \right) .
\end{aligned} \tag{31}$$

For an incomplete basis set, in general, $\langle\langle \hat{p}_\alpha^{\mathrm{gen}}; \hat{r}_\delta \rangle\rangle_\omega \neq \langle\langle \hat{p}_\delta^{\mathrm{gen}}; \hat{r}_\alpha \rangle\rangle_\omega$, which leads to an origin dependence also of the spectrum. For a complete basis set and variational methods these linear response functions are equal, as shown in App. Appendix A, which is why the length representation becomes origin independent in the basis set limit.

The explicit origin dependence of the electric-dipole–magnetic-dipole tensor in the velocity representation is

$$\langle\langle \hat{m}_\alpha^{\mathrm{gen},O+a}; \hat{p}_\beta^{\mathrm{gen},O+a} \rangle\rangle_\omega = \langle\langle \hat{m}_\alpha^{\mathrm{gen},O}; \hat{p}_\beta^{\mathrm{gen},O} \rangle\rangle_\omega + \frac{e}{2m_e} \epsilon_{\alpha\gamma\delta} a_\gamma \langle\langle \hat{p}_\delta^{\mathrm{gen},O}; \hat{p}_\beta^{\mathrm{gen},O} \rangle\rangle_\omega \tag{32}$$

and thus for the trace in Eq. (25) (note that the first term in the last line of Eq. (28) vanishes for the trace)

$$\begin{aligned}
\sum_\alpha \langle\langle \hat{m}_\alpha^{\mathrm{gen},O+a}; \hat{p}_\alpha^{\mathrm{gen},O+a} \rangle\rangle_\omega = &\sum_\alpha \langle\langle \hat{m}_\alpha^{\mathrm{gen},O}; \hat{p}_\alpha^{\mathrm{gen},O} \rangle\rangle_\omega \\
&+ \frac{e}{2m_e} \left(a_y \langle\langle \hat{p}_z^{\mathrm{gen}}; \hat{p}_x^{\mathrm{gen}} \rangle\rangle_\omega - a_z \langle\langle \hat{p}_y^{\mathrm{gen}}; \hat{p}_x^{\mathrm{gen}} \rangle\rangle_\omega \right) \\
&+ \frac{e}{2m_e} \left(a_z \langle\langle \hat{p}_x^{\mathrm{gen}}; \hat{p}_y^{\mathrm{gen}} \rangle\rangle_\omega - a_x \langle\langle \hat{p}_z^{\mathrm{gen}}; \hat{p}_y^{\mathrm{gen}} \rangle\rangle_\omega \right) \\
&+ \frac{e}{2m_e} \left(a_x \langle\langle \hat{p}_y^{\mathrm{gen}}; \hat{p}_z^{\mathrm{gen}} \rangle\rangle_\omega - a_y \langle\langle \hat{p}_x^{\mathrm{gen}}; \hat{p}_z^{\mathrm{gen}} \rangle\rangle_\omega \right) .
\end{aligned} \tag{33}$$

Since in general $\langle\langle \hat{p}_\alpha^{\mathrm{gen}}; \hat{p}_\delta^{\mathrm{gen}} \rangle\rangle_\omega = \langle\langle \hat{p}_\delta^{\mathrm{gen}}; \hat{p}_\alpha^{\mathrm{gen}} \rangle\rangle_\omega$ also holds for a finite basis set, one expects the velocity representation of the electric-dipole–magnetic-dipole tensor to be origin independent irrespective of the basis set size.

3. Computational details

The RT-TDDFT calculations presented in this work were carried out using a modified version of the package CP2K [75, 76, 77]. Its RT-TDDFT implementation [78] solves the time dependent KS equations iteratively, using the always stable predictor correlator method [79] to extrapolate the density self consistently in time. Several options are available for the calculation of the propagator and the approximation of the matrix exponential [80]. Here either the enforced time reversible symmetry or exponential midpoint method was used to calculate the propagator. For the calculation of the matrix exponential the Arnoldi subspace algorithm [81] was employed. The Gaussian and plane wave (GPW) method was used with Goedecker–Teter–Hutter (GTH) pseudo potential basis sets [82]. Additionally the Gaussian and augmented plane wave (GAPW) method [83] was used for calculations using all electron basis sets [84, 85]. All calculations were carried out using the PBE exchange–correlation functional [86].
In RT-TDDFT the form of the perturbation was chosen to be a δ-pulse, i. e. $f(t) = \delta(t)$ in Eq. (5). The perturbation in the length representation is done by using the relation [4]

$$\left|\Psi(t=0^+)\right\rangle = e^{\frac{ie}{\hbar}\vec{\kappa}\cdot\vec{r}}\left|\psi(t=0^-)\right\rangle. \tag{34}$$

which gives the required perturbation ($\vec{\kappa}$ gives the strength and direction of the pulse). For the perturbation in the velocity representation density functional perturbation theory is used on the converged ground state for the momentum operator to first order

$$\left|\phi_i^{\text{pert}}\right\rangle = \frac{ie\hbar}{m_e}\sum_{k,\text{virt}}\frac{\langle\phi_k|\kappa_\alpha\nabla_\alpha|\phi_i\rangle}{\epsilon_i-\epsilon_k}\left|\phi_k\right\rangle \tag{35}$$

where ϵ_j are the eigenvalues of the KS matrix. This is essentially the solution of Sternheimer's equation in the space of occupied and virtual groundstate orbitals. If GTH-pseudo potentials[87], which involve a non-local part, are used the momentum operator is modified according to the algebra in Eq. (15) including the commutator of the position operator with the non-local part of the pseudo potential.

This implementation of a δ-pulse in the velocity representation for the perturbation (essentially Eq. (4)) already takes care of a factor of ω in Eq. (16), so that the absorption spectrum is calculated either using Eq. (14) if the response function used is of the form $\langle\langle\hat{r};\cdot\rangle\rangle_\omega$ ('measurement' of the electric

dipole moment) or

$$S(\hbar\omega) = \frac{-2}{3\pi\hbar}\mathrm{Tr}\left\{\mathrm{Im}\left[\langle\langle\hat{p}_\alpha^{\mathrm{gen}};\cdot\rangle\rangle_\omega\right]\right\} \tag{36}$$

if the response function used is of the form $\langle\langle\hat{p}^{\mathrm{gen}};\cdot\rangle\rangle_\omega$ ('measurement' of the generalized momentum). Note that the prefactors change if a momentum perturbation is used.

During the time evolution the expectation values of several one-electron operators (electric dipole moment, magnetic dipole moment, linear momentum) are tracked simultaneously, including the commutator of the position operator with the non-local part of the pseudo potential if necessary.
For the RT-TDDFT calculations a time step of 0.1 a. u. was used for calculations using the GPW method and a time step of 0.05 a. u. for calculations with the GAPW method, since it appeared to be numerically less stable . The damping factor in Eq. (9) was set to 0.1 eV $\approx$ 0.0037 a. u. in all calculations. Each calculation was at least run for a total time of 3000 a. u.
The reference point for the position operator was set to the molecule's center of mass, if not mentioned otherwise.

4. Results and discussion

This section is structured as follows: In the first paragraph (Sec. 4.1) the different representations of the electric-dipole–electric-dipole tensor listed in Tab. 1 are examined for the calculation of the absorption spectrum of (R)-methyloxirane with respect to the inclusion of the generalized momentum, basis set dependence, and sum rules. In the second paragraph (Sec. 4.2) the same properties are evaluated for the length and velocity representation of the electric-dipole–magnetic-dipole tensor for the calculation of ECD spectra of (R)- and (S)-methyloxirane. Additionally, the origin dependence of the ECD spectrum is investigated for the different representations.

4.1. Absorption spectra

Here the different representations of the electric-dipole–electric-dipole polarizability are examined with respect to the impact of the generalized momentum in Sec. 4.1.1, the basis set dependence in Sec. 4.1.2, and sum rules in Sec. 4.1.3. Note that the first term in the last line of Eq. (16) is purely real and does not contribute to the absorption strength function in Eq. (14).

4.1.1. Representations

According to Eqs. (15) and (16) the use of the generalized momentum instead of the canonical momentum as either perturbation or observable in an RT-TDDFT calculation is vital in the presence of non-local potentials. In order to examine its influence, the absorption spectrum of (R)-methyloxirane was calculated for the aug-QZV2P-GTH basis set for different representations of the electric-dipole–electric-dipole polarizability, either including the commutator in Eq. (17) or not. The resulting spectra are shown in Fig. 1. As expected from Sec. 2.2 the linear response function has to be calculated using the generalized momentum in order to achieve an equivalent result in each of the four representations mentioned in Tab. 1. However, compared to a calculation using the canonical momentum the differences affect mostly the absolute intensities and only in rare instances also the shape of the peaks. In the language of LR-TDDFT the excitation energies are unaffected but the oscillator strengths are.

Note that we observed an offset between $\lim_{\omega\to 0} S(\hbar\omega)$ and $\lim_{\omega\to\infty} S(\hbar\omega)$ when using a representation that involves measuring either the canonical or the generalized momentum. This offset is corrected for in Fig. 1 so that the condition $\lim_{\omega\to 0} S(\hbar\omega) = 0$ is matched.

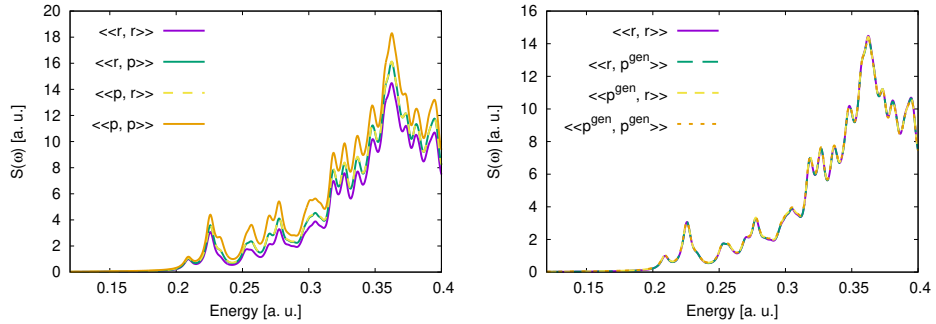

Figure 1: Absorption spectra of (R)-methyloxirane for the aug-QZV2P-GTH pseudo potential basis set calculated from different representations of the linear response function. Left hand side (LHS): Using the canonical momentum. Right hand side (RHS): Using the generalized momentum.

4.1.2. Basis set dependence

Since the change of representations is only exact for a complete basis set, a difference between the representations of the electric-dipole–electric-dipole response tensor is expected. For the aug-QZV2P-GTH basis set (see Fig. 1, RHS) this difference is barely noticeable. In order to investigate this issue the same set of calculations was carried out for the medium sized DZVP-GTH basis set. The results are shown in Fig. 2.

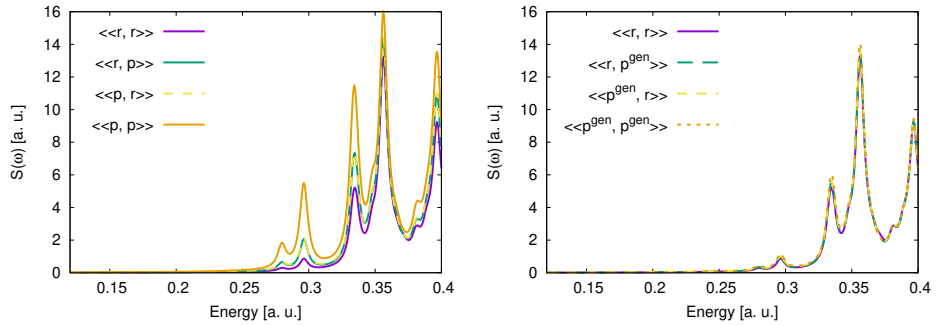

Figure 2: Absorption spectra of (R)-methyloxirane for the DZVP-GTH pseudo potential basis set calculated from different representations of the linear response function. LHS: Using the canonical momentum. RHS: Using the generalized momentum.

Again we observe rather large deviations in the absolute intensities when the canonical momentum is used while the calculations employing the generalized momentum show a more consistent picture between the different

representations in Tab. 1: Already for the DZVP-GTH basis set the differences between the length, mixed, and velocity representations are small and affect only the absolute intensities, if the generalized momentum is used. As shown in the previous section (Sec. 4.1.1) these differences can be eliminated by using an appropriately large basis set.

Another point of interest is the comparison of pseudo potential and all electron basis sets, for which $\hat{p} = \hat{p}^{\text{gen}}$. In Fig. 3 the absorption strength function is shown for the different representations of the electric-dipole–electric-dipole tensor and the aug-cc-pVQZ all electron basis set.

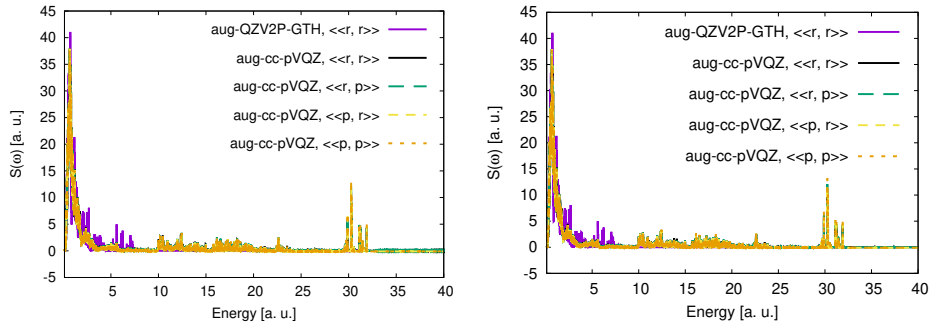

Figure 3: Absorption spectra of (R)-methyloxirane calculated for the aug-QZV2P-GTH pseudo potential and the all electron aug-cc-pVQZ basis set using different representations of the electric-dipole–electric-dipole response tensor. LHS: First few excitations. RHS: Larger energy range.

As expected for this large basis set all representations listed in Tab. 1 agree. For completeness the absorption strength function obtained with the aug-QZV2P-GTH pseudo-potential basis set is also shown and there is very good agreement between the absorption spectrum simulated with these two basis sets in excitation energy and intensity in the low frequency part. Of course, only the all electron basis set is able to capture core level excitations as e. g. necessary for the simulation of X-ray absorption spectra, as illustrated by the RHS in Fig. 3.

4.1.3. Thomas–Reiche–Kuhn sum rule

A good test for the implementation of linear response calculations in the dipole approximation [68] are sum rules. The most important one for absorption spectra is the Thomas-Reiche-Kuhn (TRK) sum rule stated in Eq. (18) (and Eq. (19) if non-local potentials are present). In RT-TDDFT the evaluations of this sum rule can be done by integrating the full spectrum (as

e. g. in the RHS of Fig. 3) numerically. In the case of non-local potentials the expectation value of the double commutator in Eq.(19) has to be taken into account. The results using the aug-cc-pVQZ all electron, the aug-QZV2P-GTH, and the DZVP-GTH pseudo potential basis sets are shown in Tab. 3.

basis set	TRK	N_e
aug-cc-pVQZ	30.37	32
aug-QZV2P-GTH	23.98	24
DZVP-GTH	24.74	24

Table 3: Evaluation of the TRK sum rule for the absorption spectrum of (R)-methyloxirane.

For the aug-cc-pVQZ all electron basis set the TRK sum rule is only approximately fulfilled. One of the reasons may be that the GAPW method appears to be numerically less stable compared to the GPW method during the real time propagation.

For the aug-QZV2P-GTH pseudo potential basis set, the TRK sum rule is very well fulfilled. The contribution of the commutator term in Eq. (19) is less than 0.05. Here also a convergence with the basis set size is observed as shown for DZVP-GTH compared to the larger aug-QZV2P-GTH basis set. Note, that the electrons included in the pseudo potential description do not appear in the sum rule.

4.2. ECD spectra

In this section the calculation of the rotatory strength function (see Eq. (25)) in RT-TDDFT is evaluated. The basis set dependence and the influence of the generalized momentum in the presence of non-local pseudo potentials are discussed. Additionally the origin dependence of the resulting spectra is examined with respect to these parameters.

4.2.1. Representations and basis set dependence

The length and velocity representation of the electric-dipole–magnetic-dipole response tensor for the calculation of the rotatory strength function in Eq. (25) are listed in Tab. 2 and related by Eq. (28). In order to investigate the impact of either using the canonical or the generalized momentum in Eq. (28), calculations were carried out for the ECD spectrum of (R)-methyloxirane and the resulting spectra for different basis sets and representations are shown in Fig. 4 for the aug-QZV2P-GTH basis set.

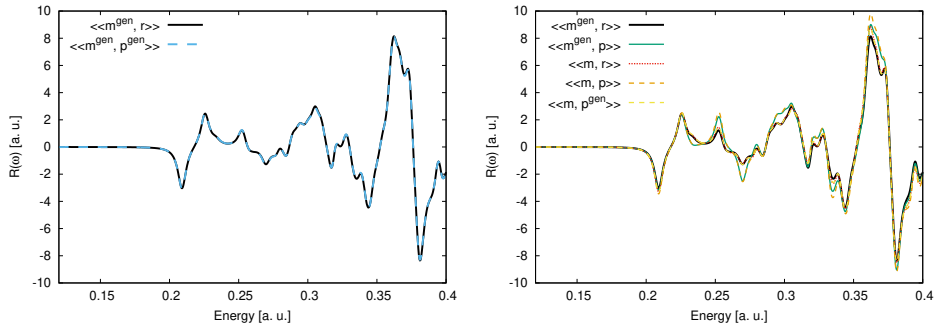

Figure 4: ECD spectrum of (R)-methyloxirane calculated in the length and velocity representation taking into account the generalized momentum (LHS) or not (RHS).

As apparent from the discussion of the theory in Sec. 2.4, the use of the generalized momentum is crucial in the presence of non-local potentials, both for achieving a gauge invariant description (see Eq. (27)) and for achieving an equivalence between the length and velocity representation according to Eq. (28). The calculations shown in Fig. 4 support this by the following points:

Firstly, there is no noticeable difference between the length and velocity representation if the generalized magnetic dipole moment is used (Eq. 27), and the generalized momentum is employed to switch between representations (Eq. (28)) (see Fig. 4, LHS).

Secondly, if the generalized momentum is neglected in the definition of the generalized magnetic dipole operator (see Eq. (27)), the spectrum shows (although small) deviations in absolute intensities in the length representation (dotted red line, RHS). This is also the case for the velocity representation including the generalized momentum (dashed bright yellow line, RHS).

Thirdly, if the generalized momentum is neglected when switching to the velocity representation (see Eq. (28)) the spectrum shows more significant differences in intensities and peak shapes even if the definition of the generalized magnetic dipole moment is used (solid green line, RHS). The same holds true also if the generalized momentum is omitted in the definition of the generalized magnetic dipole moment (see Eq. 27) (dashed orange line, RHS).

In summary, omitting the generalized momentum when switching to the velocity representation seems to have a more significant influence than omitting it in the definition of the generalized magnetic dipole moment. However, all deviations mentioned above are rather small and the spectra agree qualitatively well for this large basis set.

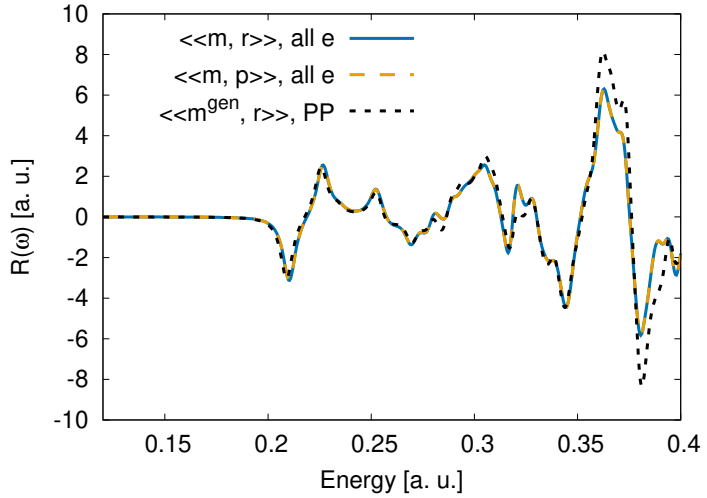

Figure 5: ECD spectrum of (R)-methyloxirane calculated in the length (solid blue) and velocity (dashed orange) representation for the aug-cc-pVQZ all electron basis set compared to the aug-QZV2P-GTH pseudo potential basis set (dotted black).

In Fig. 5, a comparison of the ECD spectrum calculated with aug-QZV2P-GTH pseudo potential basis set and the aug-cc-pVQZ all electron basis set is shown. The spectra agree qualitatively well if the generalized momentum is

used for the calculation of the electric-dipole–magnetic-dipole response tensor both for switching to the velocity representation and in the definition of the magnetic dipole moment. Also, there is no noticeable difference between the length and velocity representation using the all electron basis set, which indicates that the basis set limit is reached.

As a next step, the basis set dependence of the length and velocity representations for the ECD spectra is examined (see Fig. 6).

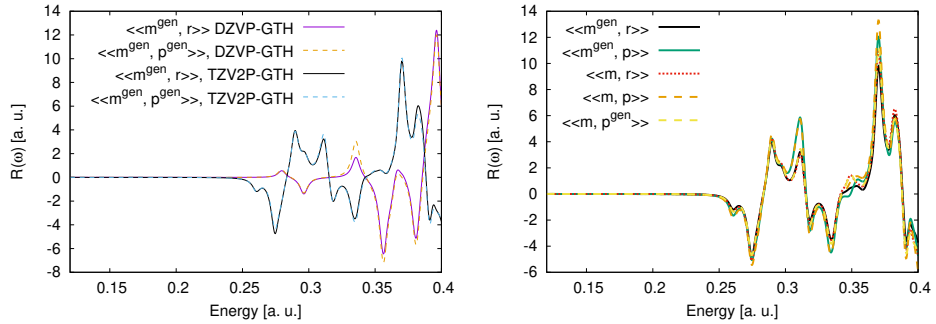

Figure 6: ECD spectrum of (R)-methyloxirane calculated in the length and velocity representation for the two different pseudo potential basis sets. LHS: Comparison of length and velocity representation for the DZVP-GTH and TZV2P-GTH basis sets respectively. RHS: ECD spectra in the TZV2P-GTH basis set if the generalized momentum is not taken into account.

It is immediately apparent that the results for both the DZVP-GTH basis set and the TZV2P-GTH basis set do not agree with the aug-QZV2P-GTH basis set concerning position, intensities and relative signs of the peaks. This suggests that a large basis set is essential for the simulation of ECD spectra.

Also the length and velocity representations taking into account the generalized momentum show noticeable differences, converging for the TZV2P-GTH basis set (Fig. 6, LHS).

Again, omitting the generalized momentum in the definition of the generalized magnetic dipole moment (see Eq. (27)) or when switching to the velocity representation (see Eq. (28)) leads to deviations in intensity (see Fig. 6, RHS), comparable to those described for Fig. 4. However, the spectra obtained in this way still agree reasonably well with each other for each respective basis set.

4.2.2. Origin dependence

As discussed in Sec. 2.4.1 the ECD spectrum calculated in the length representation and in a finite basis set is found to be origin dependent. For all electron basis sets this can be overcome by reaching for the complete basis set limit. For pseudo potential basis sets, in addition the velocity representation according to Eq. (28) and the definition of the generalized magnetic dipole moment in Eq. (27) have to be used.

The ECD spectrum for the aug-cc-pVQZ all electron basis set and the aug-QZV2P-GTH basis set for different representations and reference points is shown in Fig. 7. Note that for the all electron basis set, $\hat{m}^{\mathrm{gen}} = \hat{m}$ and that the reference point for the position operator is the molecule's center of mass (c.o.m.) placed at the center of the simulation cell, so that a reference point of $(0, 0, 0)$ represents a shift in reference point of a few $\mathring{A}$.

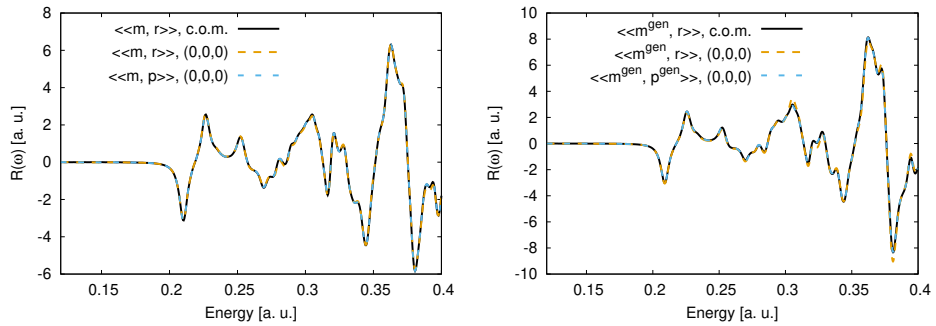

Figure 7: ECD spectrum of (R)-methyloxirane calculated for different reference points of the position operator. LHS: aug-cc-pVQZ all electron basis set. RHS: aug-QZV2P-GTH pseudo potential basis set.

Firstly, the ECD spectrum calculated with the aug-cc-pVQZ all electron basis set is origin independent irrespective of which representation is used, apart from a few barely noticeable differences in intensity. This is an indication that the basis set is approaching completeness in order to make Eq. (4) hold.

Secondly, the ECD spectrum calculated with the aug-QZV2P-GTH pseudo potential basis set taking into account the generalized momentum for switching representations in Eq. (28) and the definition of the generalized magnetic dipole moment in Eq. (27) shows only a very slight origin dependence in the length representation (dashed orange line in Fig. 7, RHS), which may also vanish by approaching the basis set limit.

In Fig. 8, ECD spectra are shown for the aug-QZV2P-GTH pseudo potential basis set and a shifted reference point of the position operator, if the generalized momentum is not taken into account, either for switching representations or in the definition of the magnetic dipole moment or both.

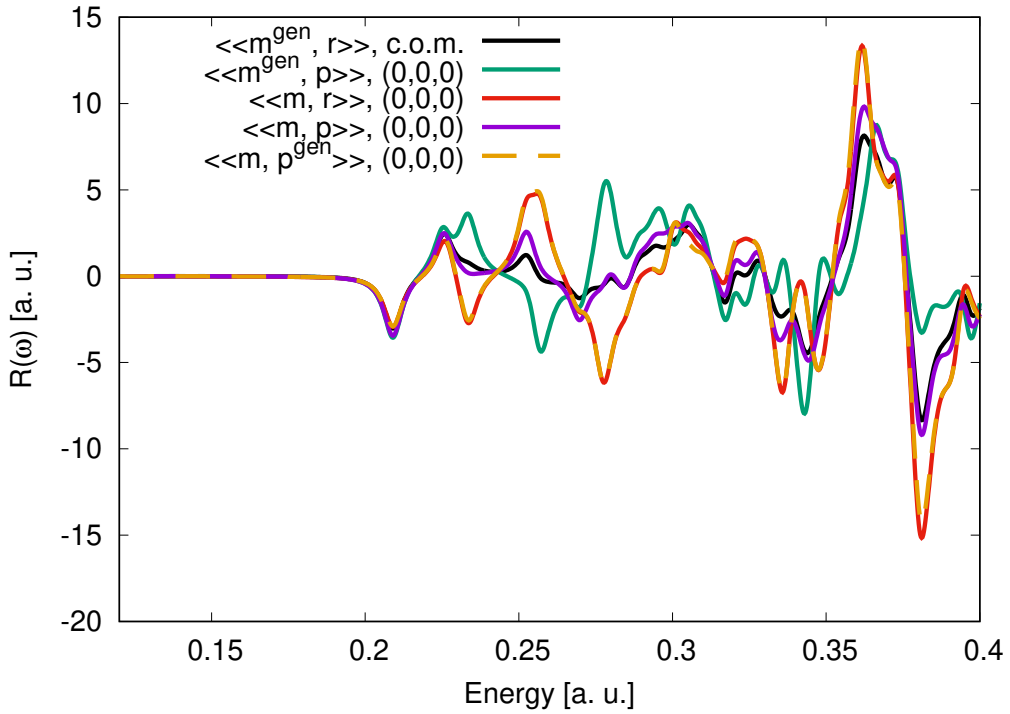

Figure 8: ECD spectrum of (R)-methyloxirane for a shifted reference point, calculated in length and velocity representations while not taking the generalized momentum into account. Basis set: aug-QZV2P-GTH.

Even if the deviations between different representations for the reference point set to the c.o.m. of the molecule were still giving qualitatively reasonable results (see Fig. 4), a shift of the reference point leads to vastly different spectra if the generalized momentum is not taken into account. Only the first peak in the spectrum can be reproduced. This means that especially for larger molecules a description according to Eq. (27) and Eq. (28) is essential in order to get meaningful ECD spectra in the presence of non-local potentials.

Note that the length (solid red line) and velocity representation (solid yellow line) while omitting the generalized momentum in the definition of

the generalized magnetic dipole moment agree rather well with each other also for the shifted origin, but show a significant origin dependence compared to the spectrum obtained with the reference point set to the c.o.m (solid black line).

These finding show that taking into account the generalized momentum both for switching to the velocity representation and in the definition of the magnetic dipole moment are crucial in order to achieve origin independent and gauge invariant ECD spectra in the presence of non-local potentials. Note that the components of the electric-dipole–magnetic-dipole tensor themselves are not origin independent, only the ECD spectrum is.

In Fig. 9 the origin dependence of the ECD spectra is shown for the smaller DZVP-GTH and TZV2P-GTH basis sets, taking the generalized momentum in Eq. (28) and in Eq. (27) into account. It is apparent, that the velocity representation (dashed orange and red lines) does not show any origin dependence as expected from Eq. (33) while the length representation (solid blue line) shows a significant origin dependence for smaller basis sets, as expected from Eq. (31).

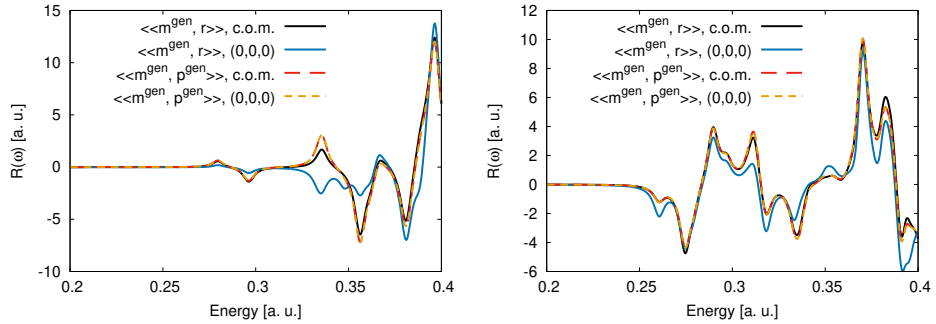

Figure 9: ECD spectrum of (R)-methyloxirane calculated in the length and velocity representation taking into account the generalized momentum for different reference points for the moment calculation. LHS: DZVP-GTH pseudo potential basis set. RHS: TZV2P-GTH pseudo potential basis set.

For completeness an ECD spectrum of both (R)- and (S)-methyloxirane are shown in Fig. 10. The ECD signals are exactly sign opposites, as expected.

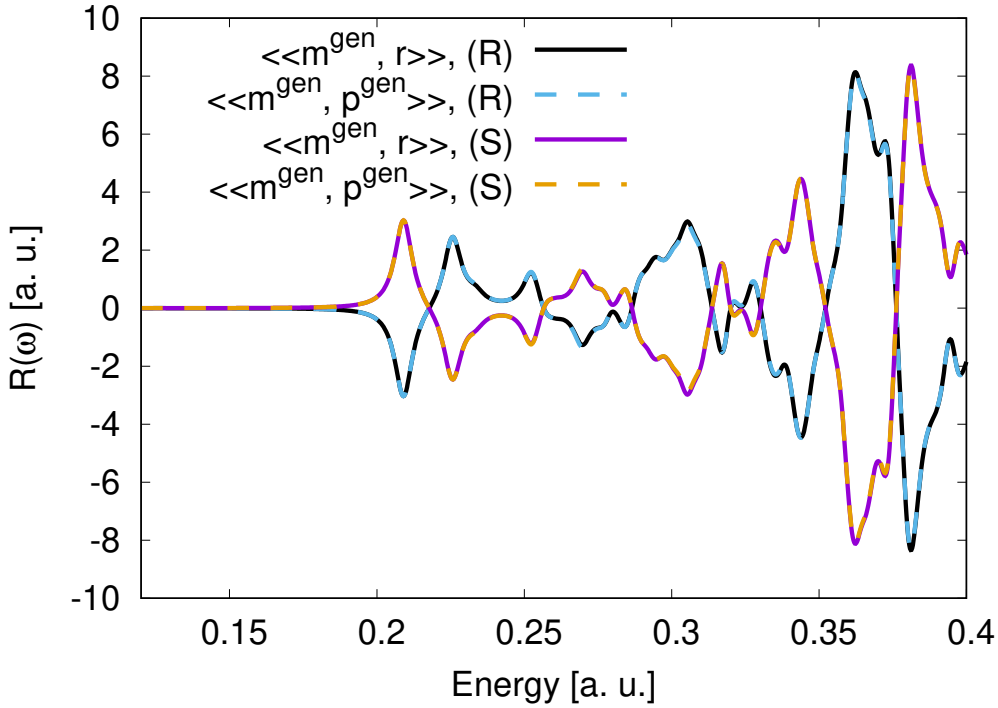

Figure 10: ECD spectrum of (R)- and (S)-methyloxirane calculated in length and velocity representations. Basis set: aug-QZV2P-GTH.

5. Conclusion

The calculation of spectroscopic (linear) response tensors was reviewed and presented in a propagator formulation in order to allow the treatment of LR- and RT-TDDFT on equal footing. Moreover differences in the meaning of length, mixed, and velocity representations, and length, and velocity gauge were pointed out. According to the propagator formalism, in the presence of non-local potentials, as e. g. the use of non-local pseudo potentials, the calculation of linear response functions in a mixed or velocity representation requires taking into account the generalized momentum, instead of the canonical momentum.

The theoretical findings were implemented and tested using the GPW and GAPW methods of the package `CP2K` and applied in the length gauge formulation of RT-TDDFT to calculate absorption and ECD spectra of (R)-methyloxirane.

For the calculation of absorption spectra (electric-dipole–electric-dipole

linear response tensor) it was found that the inclusion of the generalized momentum is vital for an equivalence of length, mixed, and velocity representations in the basis set limit using non-local pseudo potentials. Moreover, the TRK sum rule was found to be fulfilled in the basis set limit for calculations involving non-local pseudo potentials.

For the calculation of ECD spectra (electric-dipole–magnetic-dipole linear response tensor) taking the generalized momentum into account in the presence of non-local potentials is necessary for

1. the definition of the magnetic dipole moment,
2. switching to the velocity representation.

These two points are vital if an equivalence between length and velocity representation is to be achieved in the basis set limit. In addition, they are essential to obtain origin independent results in the velocity representation.

It was demonstrated that even for small basis sets an origin independent description of the ECD spectrum can be achieved in RT-TDDFT in the presence of non-local pseudo potentials, if the generalized momentum is used appropriately. In our example, the calculation of ECD spectra shows a larger basis set dependence than the calculation of absorption spectra.

In general, real time propagation provides a complementary picture to frequency domain approaches and has distinct advantages: It gives the whole frequency range in just one simulation run, is not restricted to a small energy window, and does not become significantly more difficult if the density of states increases. RT-TDDFT thus offers an attractive way to obtain ECD spectra for large systems due to its favorable scaling properties, which can be further exploited in future work.

6. Acknowledgements

This work has been supported by the University of Zurich, the university Research Priority Program "Solar Light to Chemical Energy Conversion" (LightChEC), and the Swiss National Foundation (grant no. PP00P2_170667). Our calculations have been supported by the Swiss National Supercomputing Center, accounts s745, s788, and s875.

Appendix A. Symmetry of the electric-dipole–electric-dipole response tensor

According to the equation of motion for the propagators Eq. (12) one obtains two equivalent relations between length and mixed representation of the electric-dipole–electric-dipole response tensor:

$$\hbar\omega\langle\langle\hat{r}_\alpha;\hat{r}_\beta\rangle\rangle_\omega = \frac{i\hbar}{m_e}\langle\langle\hat{p}^{\mathrm{gen}}_\alpha;\hat{r}_\beta\rangle\rangle_\omega \tag{A.1}$$

$$= -\frac{i\hbar}{m_e}\langle\langle\hat{r}_\alpha;\hat{p}^{\mathrm{gen}}_\beta\rangle\rangle_\omega. \tag{A.2}$$

Exploiting the symmetry of the electric-dipole–electric-dipole response tensor

$$\langle\langle\hat{r}_\alpha;\hat{r}_\beta\rangle\rangle_\omega = \langle\langle\hat{r}_\beta;\hat{r}_\alpha\rangle\rangle_\omega \tag{A.3}$$

one can write equivalently

$$\hbar\omega\langle\langle\hat{r}_\beta;\hat{r}_\alpha\rangle\rangle_\omega = \frac{i\hbar}{m_e}\langle\langle\hat{p}^{\mathrm{gen}}_\beta;\hat{r}_\alpha\rangle\rangle_\omega \tag{A.4}$$

$$= -\frac{i\hbar}{m_e}\langle\langle\hat{r}_\beta;\hat{p}^{\mathrm{gen}}_\alpha\rangle\rangle_\omega \tag{A.5}$$

and thus conclude that

$$\langle\langle\hat{p}^{\mathrm{gen}}_\alpha;\hat{r}_\beta\rangle\rangle_\omega = \langle\langle\hat{p}^{\mathrm{gen}}_\beta;\hat{r}_\alpha\rangle\rangle_\omega \tag{A.6}$$

$$\langle\langle\hat{r}_\alpha;\hat{p}^{\mathrm{gen}}_\beta\rangle\rangle_\omega = \langle\langle\hat{r}_\beta;\hat{p}^{\mathrm{gen}}_\alpha\rangle\rangle_\omega. \tag{A.7}$$

Since Eq. (12) only holds true for a complete basis set, Eqs. (A.6) and (A.7) approach equivalence only in the complete basis set limit.

References

[1] K. Yabana, G. F. Bertsch, Time-dependent local-density approximation in real time: Application to conjugated molecules, International Journal of Quantum Chemistry 75 (1) (1999) 55–66. doi:10.1002/(SICI)1097-461X(1999)75:1<55::AID-QUA6>3.0.CO;2-K.

[2] K. Yabana, G. F. Bertsch, Time-dependent local-density approximation in real time, Phys. Rev. B 54 (7) (1996) 4484–4487. doi:10.1103/PhysRevB.54.4484.

[3] K. Yabana, G. F. Bertsch, Approximation in Real Time : Application to Conjugated Molecules, Int. J. Quant. Chem. 75 (1999) 55–66.

[4] K. Yabana, T. Nakatsukasa, J. I. Iwata, G. F. Bertsch, Real-time, real-space implementation of the linear response time-dependent density-functional theory, Physica Status Solidi (B) Basic Research 243 (5) (2006) 1121–1138. doi:10.1002/pssb.200642005.

[5] S. Pipolo, S. Corni, R. Cammi, The cavity electromagnetic field within the polarizable continuum model of solvation: An application to the real-time time dependent density functional theory, Computational and Theoretical Chemistry 1040-1041 (2014) 112–119. doi:10.1016/j.comptc.2014.02.035.
URL http://dx.doi.org/10.1016/j.comptc.2014.02.035

[6] C. D. Pemmaraju, F. D. Vila, J. J. Kas, S. A. Sato, J. J. Rehr, K. Yabana, D. Prendergast, Velocity-gauge real-time TDDFT within a numerical atomic orbital basis set, Computer Physics Communications 226 (2018) 30–38. arXiv:1710.08573, doi:10.1016/j.cpc.2018.01.013.

[7] C. Lian, M. Guan, S. Hu, J. Zhang, S. Meng, Photoexcitation in Solids: First-Principles Quantum Simulations by Real-Time TDDFT, Advanced Theory and Simulations 1 (8) (2018) 1800055. doi:10.1002/adts.201800055.
URL http://doi.wiley.com/10.1002/adts.201800055

[8] S. Tussupbayev, N. Govind, K. Lopata, C. J. Cramer, Comparison of real-time and linear-response time-dependent density functional theories for molecular chromophores ranging from sparse to high densities of states, Journal of Chemical Theory and Computation 11 (3)

(2015) 1102–1109, pMID: 26579760. arXiv:https://doi.org/10.1021/ct500763y, doi:10.1021/ct500763y.
URL https://doi.org/10.1021/ct500763y

[9] R. Sánchez-de Armas, J. Oviedo López, M. A. San-Miguel, J. F. Sanz, P. Ordejón, M. Pruneda, Real-time td-dft simulations in dye sensitized solar cells: The electronic absorption spectrum of alizarin supported on tio2 nanoclusters, Journal of Chemical Theory and Computation 6 (9) (2010) 2856–2865, pMID: 26616086. arXiv:https://doi.org/10.1021/ct100289t, doi:10.1021/ct100289t.
URL https://doi.org/10.1021/ct100289t

[10] F. Ding, E. B. Guidez, C. M. Aikens, X. Li, Quantum coherent plasmon in silver nanowires: A real-time tddft study, The Journal of Chemical Physics 140 (24) (2014) 244705. arXiv:https://doi.org/10.1063/1.4884388, doi:10.1063/1.4884388.
URL https://doi.org/10.1063/1.4884388

[11] B. Gao, K. Ruud, Y. Luo, Plasmon resonances in linear noble-metal chains, The Journal of Chemical Physics 137 (19) (2012) 194307. arXiv:https://doi.org/10.1063/1.4766360, doi:10.1063/1.4766360.
URL https://doi.org/10.1063/1.4766360

[12] M. Thomas, F. Latorre, P. Marquetand, Resonance raman spectra of ortho-nitrophenol calculated by real-time time-dependent density functional theory, The Journal of Chemical Physics 138 (4) (2013) 044101. arXiv:https://doi.org/10.1063/1.4776218, doi:10.1063/1.4776218.
URL https://doi.org/10.1063/1.4776218

[13] F. W. Aquino, G. C. Schatz, Time-dependent density functional methods for raman spectra in open-shell systems, The Journal of Physical Chemistry A 118 (2) (2014) 517–525, pMID: 24380604. arXiv:https://doi.org/10.1021/jp411039m, doi:10.1021/jp411039m.
URL https://doi.org/10.1021/jp411039m

[14] J. Mattiat, S. Luber, Efficient calculation of (resonance) raman spectra and excitation profiles with real-time propagation, The Journal of Chemical Physics 149 (17) (2018) 174108. arXiv:https://doi.org/

10.1063/1.5051250, doi:10.1063/1.5051250.
URL https://doi.org/10.1063/1.5051250

[15] M. Thomas, S. Mühlig, T. Deckert-Gaudig, C. Rockstuhl, V. Deckert, P. Marquetand, Distinguishing chemical and electromagnetic enhancement in surface-enhanced raman spectra: The case of para-nitrothiophenol, Journal of Raman Spectroscopy 44 (11) (2013) 1497–1505. arXiv:https://onlinelibrary.wiley.com/doi/pdf/10.1002/jrs.4377, doi:10.1002/jrs.4377.
URL https://onlinelibrary.wiley.com/doi/abs/10.1002/jrs.4377

[16] D. Varsano, L. A. Espinosa-Leal, X. Andrade, M. A. L. Marques, R. di Felice, A. Rubio, Towards a gauge invariant method for molecular chiroptical properties in TDDFT, Phys. Chem. Chem. Phys. 11 (2009) 4481–4489. doi:10.1039/B903200B.

[17] J. J. Goings, X. Li, An atomic orbital based real-time time-dependent density functional theory for computing electronic circular dichroism band spectra, The Journal of Chemical Physics 144 (23) (2016) 234102. arXiv:https://doi.org/10.1063/1.4953668, doi:10.1063/1.4953668.
URL https://doi.org/10.1063/1.4953668

[18] J. J. Goings, J. M. Kasper, F. Egidi, S. Sun, X. Li, Real time propagation of the exact two component time-dependent density functional theory, The Journal of Chemical Physics 145 (10) (2016) 104107. arXiv:https://doi.org/10.1063/1.4962422, doi:10.1063/1.4962422.
URL https://doi.org/10.1063/1.4962422

[19] J. M. Kasper, P. J. Lestrange, T. F. Stetina, X. Li, Modeling L2,3-Edge X-ray Absorption Spectroscopy with Real-Time Exact Two-Component Relativistic Time-Dependent Density Functional Theory, Journal of Chemical Theory and Computation 14 (4) (2018) 1998–2006. doi:10.1021/acs.jctc.7b01279.

[20] L. Konecny, M. Kadek, S. Komorovsky, K. Ruud, M. Repisky, Resolution-of-identity accelerated relativistic two- and four-component electron dynamics approach to chiroptical spectroscopies, The Journal of Chemical Physics 149 (20) (2018) 204104. arXiv:https://doi.org/

10.1063/1.5051032, doi:10.1063/1.5051032.
URL https://doi.org/10.1063/1.5051032

[21] H. Chen, J. M. McMahon, M. A. Ratner, G. C. Schatz, Classical electrodynamics coupled to quantum mechanics for calculation of molecular optical properties: a rt-tddft/fdtd approach, The Journal of Physical Chemistry C 114 (34) (2010) 14384–14392. arXiv:https://doi.org/10.1021/jp1043392, doi:10.1021/jp1043392.
URL https://doi.org/10.1021/jp1043392

[22] T. Akama, Y. Imamura, H. Nakai, Application of real-time time-dependent density functional theory with the cvb3lyp functional to core excitations, Chemistry Letters 39 (4) (2010) 407–409. arXiv:https://doi.org/10.1246/cl.2010.407, doi:10.1246/cl.2010.407.
URL https://doi.org/10.1246/cl.2010.407

[23] A. J. Lee, F. D. Vila, J. J. Rehr, Local time-correlation approach for calculations of x-ray spectra, Phys. Rev. B 86 (2012) 115107. doi:10.1103/PhysRevB.86.115107.
URL https://link.aps.org/doi/10.1103/PhysRevB.86.115107

[24] K. Lopata, B. E. Van Kuiken, M. Khalil, N. Govind, Linear-response and real-time time-dependent density functional theory studies of core-level near-edge x-ray absorption, Journal of Chemical Theory and Computation 8 (9) (2012) 3284–3292, pMID: 26605735. arXiv:https://doi.org/10.1021/ct3005613, doi:10.1021/ct3005613.
URL https://doi.org/10.1021/ct3005613

[25] M. Kadek, L. Konecny, B. Gao, M. Repisky, K. Ruud, X-ray absorption resonances near L<inf>2,3</inf>-edges from real-time propagation of the Dirac-Kohn-Sham density matrix, Physical Chemistry Chemical Physics 17 (35) (2015) 22566–22570. doi:10.1039/c5cp03712c.

[26] S. A. Fischer, C. J. Cramer, N. Govind, Excited state absorption from real-time time-dependent density functional theory, Journal of Chemical Theory and Computation 11 (9) (2015) 4294–4303, pMID: 26575924. arXiv:https://doi.org/10.1021/acs.jctc.5b00473, doi:10.1021/acs.jctc.5b00473.
URL https://doi.org/10.1021/acs.jctc.5b00473

[27] D. Cho, J. R. Rouxel, M. Kowalewski, P. Saurabh, J. Y. Lee, S. Mukamel, Phase cycling rt-tddft simulation protocol for nonlinear xuv and x-ray molecular spectroscopy, The Journal of Physical Chemistry Letters 9 (5) (2018) 1072–1078, pMID: 29431442. arXiv:https://doi.org/10.1021/acs.jpclett.8b00061, doi:10.1021/acs.jpclett.8b00061.
URL https://doi.org/10.1021/acs.jpclett.8b00061

[28] M. R. Provorse, C. M. Isborn, Electron dynamics with real-time time-dependent density functional theory, International Journal of Quantum Chemistry 116 (10) (2016) 739–749. arXiv:https://onlinelibrary.wiley.com/doi/pdf/10.1002/qua.25096, doi:10.1002/qua.25096.
URL https://onlinelibrary.wiley.com/doi/abs/10.1002/qua.25096

[29] J. J. Goings, P. J. Lestrange, X. Li, Real-time time-dependent electronic structure theory, Wiley Interdisciplinary Reviews: Computational Molecular Science 8 (1) (2018) e1341. arXiv:https://onlinelibrary.wiley.com/doi/pdf/10.1002/wcms.1341, doi:10.1002/wcms.1341.
URL https://onlinelibrary.wiley.com/doi/abs/10.1002/wcms.1341

[30] C. J. Pickard, F. Mauri, All-electron magnetic response with pseudopotentials: NMR chemical shifts 63 (2001) 1–13. arXiv:0101257, doi:10.1103/PhysRevB.63.245101.
URL http://arxiv.org/abs/cond-mat/0101257{%}0Ahttp://dx.doi.org/10.1103/PhysRevB.63.245101

[31] C. J. Pickard, F. Mauri, Nonlocal pseudopotentials and magnetic fields, Physical Review Letters 91 (19) (2003) 7–10. arXiv:0304115, doi:10.1103/PhysRevLett.91.196401.

[32] F. Ding, W. Liang, C. T. Chapman, C. M. Isborn, X. Li, On the gauge invariance of nonperturbative electronic dynamics using the time-dependent Hartree-Fock and time-dependent Kohn-Sham, Journal of Chemical Physics 135 (16). doi:10.1063/1.3655675.

[33] F. London, Théorie quantique des courants interatomiques dans les combinaisons aromatiques, J. Phys. Radium 8 (10) (1937) 397–409. doi:10.1051/jphysrad:01937008010039700.
URL https://hal.archives-ouvertes.fr/jpa-00233534

[34] K. L. Bak, A. E. Hansen, K. Ruud, T. Helgaker, J. Olsen, P. Jørgensen, Ab initio calculation of electronic circular dichroism for trans-cyclooctene using london atomic orbitals, Theoretica chimica acta 90 (5) (1995) 441–458. doi:10.1007/BF01113546.
URL https://doi.org/10.1007/BF01113546

[35] A. M. Lee, N. C. Handy, S. M. Colwell, The density functional calculation of nuclear shielding constants using london atomic orbitals, The Journal of Chemical Physics 103 (23) (1995) 10095–10109. arXiv:https://doi.org/10.1063/1.469912, doi:10.1063/1.469912.
URL https://doi.org/10.1063/1.469912

[36] M. Pecul, K. Ruud, T. Helgaker, Density functional theory calculation of electronic circular dichroism using london orbitals, Chemical Physics Letters 388 (1) (2004) 110 – 119. doi:https://doi.org/10.1016/j.cplett.2004.03.008.
URL http://www.sciencedirect.com/science/article/pii/S0009261404003318

[37] T. B. Pedersen, H. Koch, L. Boman, A. M. Sánchez De Merás, Origin invariant calculation of optical rotation without recourse to London orbitals, Chemical Physics Letters 393 (4-6) (2004) 319–326. doi:10.1016/j.cplett.2004.06.065.

[38] S. Chandrasekhar, On the continuous absorption coefficient of the negative hydrogen ion, Astrophysical Journal 102 (1945) 223–231. doi:10.1086/144755.

[39] H. A. Bethe, E. E. Salpeter, Quantum Mechanics of One- and Two-Electron Atoms, Springer, Berlin, Heidelberg, 1957. doi:10.1007/978-3-662-12869-5.

[40] J. C. Y. Chen, Offdiagonal hypervirial theorem and its applications, The Journal of Chemical Physics 40 (3) (1964) 615–621. arXiv:https:

//doi.org/10.1063/1.1725180, doi:10.1063/1.1725180.
URL https://doi.org/10.1063/1.1725180

[41] A. E. Hansen, On the equivalence of different hamiltonians for the semi-classical radiation theory, Theoretica chimica acta 16 (3) (1970) 217–225. doi:10.1007/BF00527566.
URL https://doi.org/10.1007/BF00527566

[42] H. Paul, J. Frahm, Strungstheoretische quivalenz der wechselwirkungsoperatoren hw =e/mc + e2/2mc22 und w =, Annalen der Physik 474 (34) (1967) 216–224. arXiv:https://onlinelibrary.wiley.com/doi/pdf/10.1002/andp.19674740313, doi:10.1002/andp.19674740313.
URL https://onlinelibrary.wiley.com/doi/abs/10.1002/andp.19674740313

[43] C. A. Nicolaides, D. R. Beck, On the length, velocity and acceleration expressions for the calculation of accurate oscillator strengths in many-electron systems, Chemical Physics Letters 35 (2) (1975) 202 – 209. doi:https://doi.org/10.1016/0009-2614(75)85314-0.
URL http://www.sciencedirect.com/science/article/pii/0009261475853140

[44] S. Luber, M. Reiher, Raman optical activity spectra of chiral transition metal complexes, Chemical Physics 346 (1) (2008) 212 – 223. doi:https://doi.org/10.1016/j.chemphys.2008.01.046.
URL http://www.sciencedirect.com/science/article/pii/S0301010408000621

[45] S. Luber, Raman optical activity spectra from density functional perturbation theory and density-functional-theory-based molecular dynamics, Journal of Chemical Theory and Computation 13 (3) (2017) 1254–1262, pMID: 28218847. arXiv:https://doi.org/10.1021/acs.jctc.6b00820, doi:10.1021/acs.jctc.6b00820.
URL https://doi.org/10.1021/acs.jctc.6b00820

[46] S. Luber, J. Neugebauer, M. Reiher, Enhancement and de-enhancement effects in vibrational resonance raman optical activity, The Journal of Chemical Physics 132 (4) (2010) 044113. arXiv:https://doi.org/10.

1063/1.3300069, doi:10.1063/1.3300069.
URL https://doi.org/10.1063/1.3300069

[47] D. H. Kobe, Gauge-invariant resolution of the controversy over length versus velocity forms of the interaction with electric dipole radiation, Phys. Rev. A 19 (1979) 205–214. doi:10.1103/PhysRevA.19.205.
URL https://link.aps.org/doi/10.1103/PhysRevA.19.205

[48] D. H. Kobe, Question of gauge: Nonresonant two-photon absorption, Phys. Rev. Lett. 40 (1978) 538–540. doi:10.1103/PhysRevLett.40.538.
URL https://link.aps.org/doi/10.1103/PhysRevLett.40.538

[49] D. H. Kobe, A. L. Smirl, Gauge invariant formulation of the interaction of electromagnetic radiation and matter, American Journal of Physics 46 (6) (1978) 624–633. arXiv:https://doi.org/10.1119/1.11264, doi:10.1119/1.11264.
URL https://doi.org/10.1119/1.11264

[50] D. H. Kobe, Gauge transformations and the electric dipole approximation, American Journal of Physics 50 (2) (1982) 128–133. arXiv:https://doi.org/10.1119/1.13029, doi:10.1119/1.13029.
URL https://doi.org/10.1119/1.13029

[51] D. H. Kobe, K.-H. Yang, Gauge transformation of the time-evolution operator, Phys. Rev. A 32 (1985) 952–958. doi:10.1103/PhysRevA.32.952.
URL https://link.aps.org/doi/10.1103/PhysRevA.32.952

[52] A. F. Starace, Length and Velocity Formulas in Approximate Oscillator-Strength Calculations, Phys. Rev. A 3 (4) (1971) 1242–1245. doi:https://doi.org/10.1103/PhysRevA.3.1242.

[53] D. L. Lin, Velocity and length forms of oscillator strengths and unitary transformations of quantum electrodynamics, Phys. Rev. A 17 (1978) 1939–1943. doi:10.1103/PhysRevA.17.1939.
URL https://link.aps.org/doi/10.1103/PhysRevA.17.1939

[54] J. Linderberg, Y. Öhrn, Propagators in Quantum Chemistry, John Wiley & Sons, 2004.

[55] J. Olsen, P. Jørgensen, Linear and nonlinear response functions for an exact state and for an mcscf state, The Journal of Chemical Physics 82 (7) (1985) 3235–3264. arXiv:https://doi.org/10.1063/1.448223, doi:10.1063/1.448223.
URL https://doi.org/10.1063/1.448223

[56] J. Jensen, A. R. Mackintosh, Rare Earth Magnetism: Structures and Excitations, Clarendon Press, Oxford, 1991.

[57] R. Kubo, Statistical-Mechanical Theory of Irreversible Processes. I., J. Phys. Soc. Jpn. 12 (6) (1957) 570–586. doi:https://doi.org/10.1143/JPSJ.12.570.

[58] M. E. Casida, Time-Dependent Density Functional Response Theory for Molecules, Vol. 1, World Scientific, 1995.

[59] R. M. Sternheimer, Electronic polarizabilities of ions from the hartree-fock wave functions, Phys. Rev. 96 (1954) 951–968. doi:10.1103/PhysRev.96.951.
URL https://link.aps.org/doi/10.1103/PhysRev.96.951

[60] P. Jørgensen, J. Oddershede, N. H. Beebe, Polarization propagator calculations of frequency-dependent polarizabilities, Verdet constants, and energy weighted sum rules, The Journal of Chemical Physics 68 (6) (1978) 2527–2532. doi:10.1063/1.436111.

[61] T. Helgaker, K. Ruud, K. L. Bak, P. Jørgensen, J. Olsen, Vibrational Raman optical activity calculations using London atomic orbitals, Faraday Discussions 99 (1994) 165–180. doi:10.1039/FD9949900165.

[62] K. Yabana, G. F. Bertsch, Application of the time-dependent local density approximation to optical activity, Physical Review A 60 (2) (1999) 1271–1279. arXiv:9812019, doi:10.1103/PhysRevA.60.1271.
URL http://link.aps.org/doi/10.1103/PhysRevA.60.1271

[63] S. Mukamel, Principles of Nonlinear Optical Spectroscopy, Oxford University Press, Oxford, 1999.

[64] F. Furche, On the density matrix based approach to time-dependent density functional response theory, Journal of Chemical Physics 114 (14) (2001) 5982–5992. doi:10.1063/1.1353585.

[65] K.-H. Yang, Gauge transformations and quantum mechanics i. gauge invariant interpretation of quantum mechanics, Annals of Physics 101 (1) (1976) 62 – 96. doi:https://doi.org/10.1016/0003-4916(76)90275-X.
URL http://www.sciencedirect.com/science/article/pii/000349167690275X

[66] M. Göppert-Mayer, Über Elementarakte mit zwei Quantensprüngen, Annalen der Physik 401 (3) (1931) 273–294. doi:10.1002/andp.19314010303.
URL https://onlinelibrary.wiley.com/doi/abs/10.1002/andp.19314010303

[67] L. Boßmann, R. Grummt, M. Kolb, On the dipole approximation with error estimates, Letters in Mathematical Physics 108 (1) (2018) 185–193. doi:10.1007/s11005-017-0999-y.
URL https://doi.org/10.1007/s11005-017-0999-y

[68] P. J. Lestrange, F. Egidi, X. Li, The consequences of improperly describing oscillator strengths beyond the electric dipole approximation, The Journal of Chemical Physics 143 (23) (2015) 234103. arXiv:https://doi.org/10.1063/1.4937410, doi:10.1063/1.4937410.
URL https://doi.org/10.1063/1.4937410

[69] L. D. Barron, Molecular Light Scattering and Optical Activity, Cambridge University Press, Cambridge, 1982.

[70] S. Ismail-Beigi, E. K. Chang, S. G. Louie, Coupling of nonlocal potentials to electromagnetic fields, Physical Review Letters 87 (8) (2001) 87402–1–87402–4. arXiv:0101383, doi:10.1103/PhysRevLett.87.087402.

[71] X. Andrade, D. Strubbe, U. De Giovannini, A. H. Larsen, M. J. Oliveira, J. Alberdi-Rodriguez, A. Varas, I. Theophilou, N. Helbig, M. J. Verstraete, L. Stella, F. Nogueira, A. Aspuru-Guzik, A. Castro, M. A. Marques, A. Rubio, Real-space grids and the Octopus code as tools for the development of new simulation approaches for electronic systems, Physical Chemistry Chemical Physics 17 (47) (2015) 31371–31396. doi:10.1039/c5cp00351b.

[72] M. Schindler, W. Kutzelnigg, Theory of magnetic susceptibilities and nmr chemical shifts in terms of localized quantities. ii. application to some simple molecules, The Journal of Chemical Physics 76 (4) (1982) 1919–1933. arXiv:https://doi.org/10.1063/1.443165, doi:10.1063/1.443165.
URL https://doi.org/10.1063/1.443165

[73] K. Wolinski, J. F. Hinton, P. Pulay, Efficient implementation of the gauge-independent atomic orbital method for nmr chemical shift calculations, Journal of the American Chemical Society 112 (23) (1990) 8251–8260. arXiv:https://doi.org/10.1021/ja00179a005, doi:10.1021/ja00179a005.
URL https://doi.org/10.1021/ja00179a005

[74] L. A. Nafie, Velocitygauge formalism in the theory of vibrational circular dichroism and infrared absorption, The Journal of Chemical Physics 96 (8) (1992) 5687–5702. arXiv:https://doi.org/10.1063/1.462668, doi:10.1063/1.462668.
URL https://doi.org/10.1063/1.462668

[75] CP2K version 6.1 (Developement Version), the cp2k developers group (2019); available from http://www.cp2k.org.

[76] J. Vandevondele, M. Krack, F. Mohamed, M. Parrinello, T. Chassaing, J. Hutter, Quickstep: Fast and accurate density functional calculations using a mixed Gaussian and plane waves approach, Computer Physics Communications 167 (2) (2005) 103–128. doi:10.1016/j.cpc.2004.12.014.

[77] J. Hutter, M. Iannuzzi, F. Schiffmann, J. Vandevondele, Cp2k: Atomistic simulations of condensed matter systems, Wiley Interdisciplinary Reviews: Computational Molecular Science 4 (1) (2014) 15–25. arXiv:9512004, doi:10.1002/wcms.1159.

[78] S. Andermatt, J. Cha, F. Schiffmann, J. VandeVondele, Combining linear-scaling DFT with subsystem DFT in born-oppenheimer and ehrenfest molecular dynamics simulations: From molecules to a virus in solution, Journal of Chemical Theory and Computation 12 (7) (2016) 3214–3227. doi:10.1021/acs.jctc.6b00398.

[79] J. Kolafa, Numerical integration of equations of motion with a self-consistent field given by an implicit equation, Molecular Simulation 18 (3) (1996) 193–212. arXiv:https://doi.org/10.1080/08927029608024123, doi:10.1080/08927029608024123.
URL https://doi.org/10.1080/08927029608024123

[80] C. Moler, C. Van Loan, Nineteen dubious ways to compute the exponential of a matrix, twenty-five years later, SIAM Review 45 (1) (2003) 3–49. arXiv:https://doi.org/10.1137/S00361445024180, doi:10.1137/S00361445024180.
URL https://doi.org/10.1137/S00361445024180

[81] W. E. Arnoldi, The principle of minimized iterations in the solution of the matrix eigenvalue problem, Quarterly of Applied Mathematics 9 (1) (1951) 17–29. doi:10.1090/qam/42792.

[82] J. VandeVondele, J. Hutter, Gaussian basis sets for accurate calculations on molecular systems in gas and condensed phases, Journal of Chemical Physics 127 (11). doi:10.1063/1.2770708.

[83] G. Lippert, J. Hutter, M. Parrinello, The gaussian and augmented-plane-wave density functional method for ab initio molecular dynamics simulations, Theoretical Chemistry Accounts 103 (2) (1999) 124–140. doi:10.1007/s002140050523.
URL https://doi.org/10.1007/s002140050523

[84] T. H. Dunning, Gaussian basis sets for use in correlated molecular calculations. i. the atoms boron through neon and hydrogen, The Journal of Chemical Physics 90 (2) (1989) 1007–1023. arXiv:https://doi.org/10.1063/1.456153, doi:10.1063/1.456153.
URL https://doi.org/10.1063/1.456153

[85] D. E. Woon, T. H. Dunning, Gaussian basis sets for use in correlated molecular calculations. iii. the atoms aluminum through argon, The Journal of Chemical Physics 98 (2) (1993) 1358–1371. arXiv:https://doi.org/10.1063/1.464303, doi:10.1063/1.464303.
URL https://doi.org/10.1063/1.464303

[86] J. P. Perdew, K. Burke, M. Ernzerhof, Generalized gradient approximation made simple, Phys. Rev. Lett. 77 (1996) 3865–3868. doi:

10.1103/PhysRevLett.77.3865.
URL https://link.aps.org/doi/10.1103/PhysRevLett.77.3865

[87] S. Goedecker, M. Teter, J. Hutter, Separable dual-space gaussian pseudopotentials, Phys. Rev. B 54 (1996) 1703–1710. doi:10.1103/PhysRevB.54.1703.
URL https://link.aps.org/doi/10.1103/PhysRevB.54.1703